SAND2019-8510C

Uncertainty Analysis for Transverse Surface Velocity Measurements

Jeff W. LaJeunesse[1, a)], Peter A. Sable[2, b)], John P. Borg[2, c)]

[1]Sandia National Laboratories, Albuquerque, NM, 87123, USA
[2]Marquette University, Milwaukee, WI, 53233, USA

[a)]jwlajeu@sandia.gov
[b)]peter.sable@marquette.edu
[c)]john.borg@marquette.edu

Abstract. Transverse surface velocity measurements are fundamental to performing pressure-shear plate impact experiments. Recent works have utilized slight variations of traditional velocimetry techniques that measure apparent velocity from a combination of fiber optic probes aligned at non-zero angles relative to a surface normal. Various methods involving active and/or passive angled probes are proposed. This work compares the uncertainty in each approach using a multi-component velocity test case and explores the influence of parameters such as probe angle relative to the surface normal, impact angle, and measurement uncertainty of the velocimetry system. Recommendations for optimal configuration are presented. Sandia National Laboratories is a multi-mission laboratory managed and operated by National Technology & Engineering Solutions of Sandia, LLC, a wholly owned subsidiary of Honeywell International Inc., for the U.S. Department of Energy's National Nuclear Security Administration under contract DE-NA0003525.

INTRODUCTION

Transverse surface velocity measurements are of interest to variety of fields, particularly within the dynamic material properties community. Their most common use lies in pressure-shear plate impact experiments, which rely on an observation of both longitudinal and transverse surface velocity components to determine normal and shear wave propagation in target materials. This combined normal-shear wave propagation is indicative of the loading state and an accurate stress measurements dependent directly on the uncertainty within the normal and transverse velocity measurement. Previous works established a technique called TDI in which a diffraction grating is vapor deposited onto the rear surface of a target anvil [1, 2]. Either VISAR (Velocity Interferometer for Any Reflective Surface [3]) or PDV (Photon Doppler Velocimetry [4]) probes are then aligned both parallel and angled relative to the surface normal. The angled probes track the motion of first order diffraction grating fringes and relate it to transverse surface motion through the spacing of grating peaks. This technique has successfully been utilized for many experimental efforts, but requires significant surface preparation for each target anvil.

More recent works [5-11] have built on traditional velocimetry techniques by adding an angled probe to observe a component of transverse surface velocity. Light return on angled probes is accomplished by treating the target free surface with a linearly diffuse pattern that allows specular, diffuse, and retroreflective light return at both normal and non-normal angles. A variety of probe (PDV collimator) configurations have been explored, but their uncertainties less characterized. Most configurations require a small component of transverse velocity to be calculated from two, much larger, apparent velocities. This work establishes six types of PDV configurations that can be used to accomplish this and determines geometric advantages amongst them by comparing their relative uncertainty in calculated transverse surface velocity.

PDV operates by emitting single wavelength laser light from a fiber optic collimator onto a reflective surface. As the reflective surface begins to move, the reflected laser light is Doppler shifted and recollected by the

collimator. The Doppler shifted light is then combined with original light, creating a beat frequency that can be digitized using photo receivers. The beat frequency can then be related to surface velocity using the equation

$$v^* = \frac{1}{2}(f_b - f_0)\lambda_{Laser} \tag{1}$$

where v^* is the apparent velocity, f_b is the beat frequency digitized by the photo receiver, f_0 is the reference frequency of the original light, and λ_{Laser} is the wavelength of the original laser light.

Traditional PDV setups utilize a single collimator aligned perpendicular to the reflective surface, which then measures the component of velocity normal to the reflective surface. However, to observe a component of the transverse surface velocity, collimators need to be aligned at non-normal angles to the surface. This introduces a wide variety of choices when setting up a transverse surface velocity measurement system. Probes aligned at non-normal angles to the surface will be referred to as "angled" in this work. Likewise, probes aligned normal to the surface will be referred to as "normal." Next, measurements can be made using probes that are emitting and collecting light (active) or not emitting and only collecting light (passive). Passive probes can make apparent velocity measurements by collecting light from other active probes. Figure 1 depicts a scenario in which multiple velocity components of a planar surface is observed using a passive probe, R (receive), and an active probe, S (send).

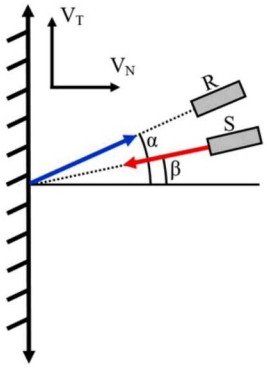

FIGURE 1 Planar surface with velocity components in both the i- and j-direction.

The apparent velocity, V*, as observed by probe R, is given by:

$$V^* = \frac{V_N}{2}(cos\alpha + cos\beta) + \frac{V_T}{2}(sin\alpha + sin\beta) + \frac{V_E}{2}(sin\gamma + sin\emptyset) \tag{2}$$

where V_N, V_T, and V_E are the normal, transverse, and out of plane components of velocity, respectively. Angles α and β are measured relative to the surface normal and correspond to probe R and S, respectively. Angles γ and $\emptyset$ are the associated with the misalignment of probes R and S, but also with any out-of-plane velocity components. In the context of pressure-shear experiments, if impact tilt is negligible, out of plane velocity, V_E, will be negligible. Likewise, if the probes are aligned accurately along a plane normal to the reflective surface (and parallel to the transverse surface motion), γ and $\emptyset$ will be zero and the last term in equation 2 can be neglected. However, their effects can be investigated with an estimate of out-of-plane velocity, which requires a thorough understanding of three-dimensional tilt effects, and a general approach to quantify the uncertainty in transverse surface velocity. For the purposes of this work, the out-of-plane velocity is assumed to be zero.

METHODOLOGY

The following section will describe a series of probe configurations that can be utilized to make simultaneous normal and transverse surface velocity measurements. Six distinct configurations were identified to form a basis of comparison, each of which can be further expanded and modified based on available components and measurement accuracy requirements. All six cases utilize an active normal probe, which directly measures the normal component of velocity as well as supplies light for any angled probes.

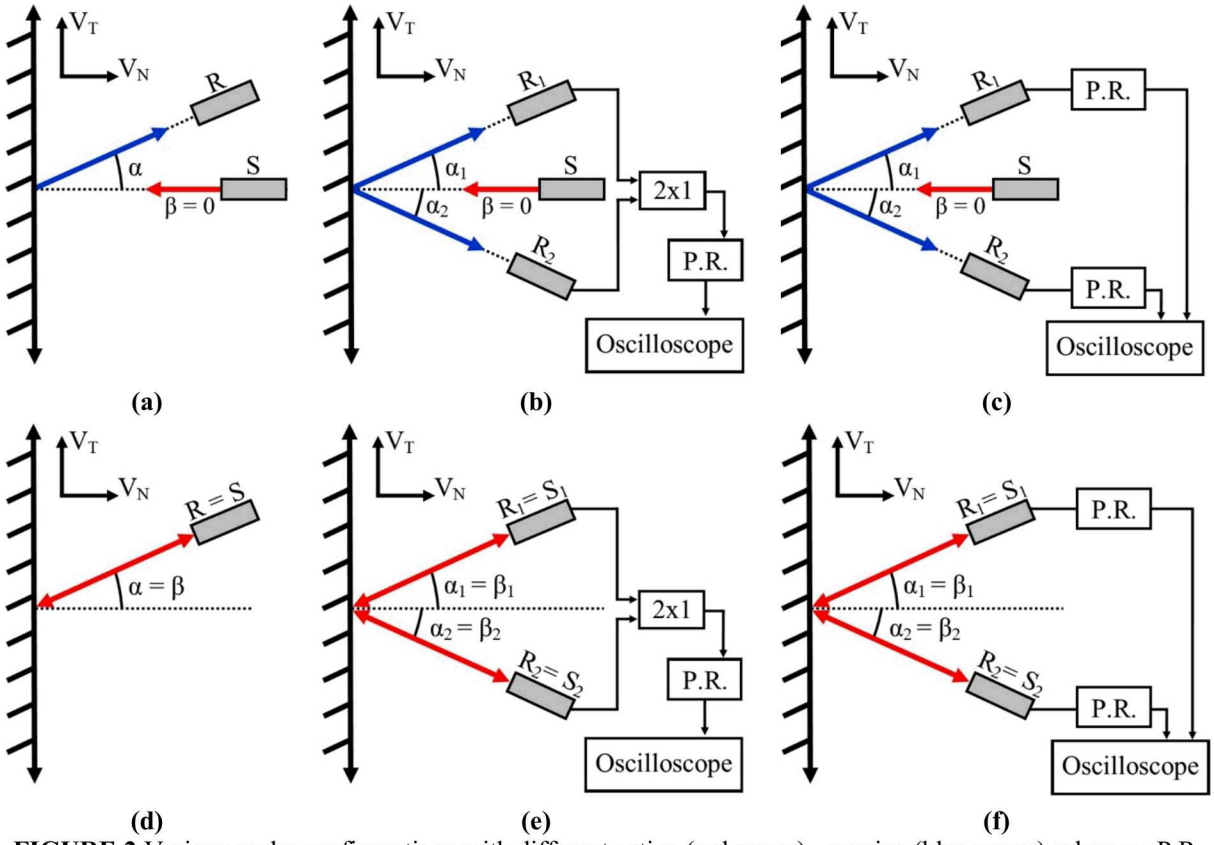

FIGURE 2 Various probe configurations with different active (red arrow) - passive (blue arrow) schemes. P.R. = Photo Receiver. Note: An active normal collimator is needed for each case, but is not shown for 2a, 2b, or 2c to demonstrate where the received on the angled collimators originated.

Three cases have passive-angled probes that only collected diffusely reflected light originally emitted from the active-normal probe, i.e. $\beta = 0$ and $\alpha \neq 0$, figure 2A, 2B, 2C. The remaining cases utilize active-angled probes that both emit and retro-reflectively collect their own light, i.e. $\alpha = \beta \neq 0$, figure 2D, 2E, 2F. The set of six configurations is then separated into three final sets. First, a single measurement configuration with a normal-active probe and an angled probe, figure 2A and 2D. Second, a direct measurement configuration with two angled probes that are combined prior to being sent to the photo receiver, figure 2B and 2E. This technique was developed by Zuanetti et al [7] and uses a clever cancelation of the observed normal component of velocity, which results in the observed velocity being directly proportional to transverse velocity. Third, an averaged configuration that uses a pair of angled probes to make individual measurements of apparent velocity, calculate a transverse velocity for each, and then averages them to obtain a final transverse velocity, figure 1C and 1F. The difference between direct and averaged measurement configurations is the combination of signals before the photo receiver in the direct measurement. Table 1 summarizes the transverse velocity equations for each configuration. Note, V_N is the normal velocity as observed on the normal probe, V^* is the apparent velocity as observed on an angled probe, and V_T is the transverse velocity either directly measured or calculated from V_N and V^*.

The primary metric for comparing each probe configuration was the relative uncertainty in transverse velocity, $\delta V_T / V_T$. To accomplish this, uncertainty propagation was performed on the transverse velocity equation associated with each probe configuration to calculate δV_T. Synthetic data consisting of a symmetric pressure-shear plate impact experiment with apparent, V^*, and normal velocity, V_N, components was then fed into the transverse velocity uncertainty model. A symmetric impact such as this allows the expected (final) components of normal and transverse free surface particle velocity, u_{FS} and v_{FS}, to be calculated, without any dependence on material density or sound speed and assuming both the flyer and target remain elastic, directly from the initial velocity, V_0, and impact angle, θ, as $u_{FS} = V_N = V_0 cos\theta$ and $v_{FS} = V_T = V_0 sin\theta$.

TABLE 1 Transverse Velocity Equations for each of the Six Probe Configurations

Configuration	Probe Angles	Transverse Velocity Equation
Single Measurement Passive Angled Probe	$\beta = 0;\ \alpha \neq 0$	$V_T = \frac{1}{sin\alpha}\left(2V^* - V_N(cos\alpha + 1)\right)$
Single Measurement Active Angled Probe	$\beta = \alpha \neq 0$	$V_T = \frac{1}{sin\alpha}(V^* - V_N cos\alpha)$
Direct Measurement Passive Angled Probes	$\beta_1 = \beta_2 = 0;\ \alpha_1 = \alpha;\ \alpha_2 = -\alpha;$	$V_T = \frac{V_1^* - V_2^*}{sin\alpha}$
Direct Measurement Active Angled Probes	$\beta_1 = \alpha_1 = \alpha;\ \beta_2 = \alpha_2 = -\alpha;$	$V_T = \frac{V_1^* - V_2^*}{2sin\alpha_1} = \frac{V_1^* - V_2^*}{2sin\alpha_2}$
Averaged Measurement Active Angled Probes	$\beta = 0;\ \alpha_1 = \alpha;\ \alpha_2 = -\alpha;$	$V_T = \frac{V_{T,1} + V_{T,2}}{2}$
Averaged Measurement Active Angled Probes	$\beta_1 = \alpha_1 = \alpha;\ \beta_2 = \alpha_2 = -\alpha;$	$V_T = \frac{V_{T,1} + V_{T,2}}{2}$

Uncertainty propagation performed on the transverse velocity equations involved by first determining the uncertainty contribution from each independent variable and then summing them in quadrature. The reduced form of uncertainty for single measurements is provided in equation 2, direct measurements in equation 3, and averaged measurements in equation 4. The general forms of these equations were then used in a parameter study that varied impact angle, θ, from 15 – 25 degrees, collimator angle, α & β, from 0 – 90 degrees, and measurement uncertainty in particle velocity for a given probe, δV_N & δV^*, from 1, 2, and 5 percent magnitude, i.e. $\delta V_N = 0.01 V_N$. An initial velocity of 100 m/s was chosen based on typical expected impact velocities in pressure-shear plate impact experiments. The out-of-plane component of velocity, V_E, and angles, γ and $\emptyset$, were assumed to be zero, i.e. negligible impact tilt and no out-of-plane alignment of the angled probes. The uncertainty in probe angle was set to $\delta\alpha = 0.1^o$ for all angles based on feasible measurement accuracy. Only first order interference was considered for configurations with active angled probes. Therefore, if any additional "cross-talk" between probes occurred, e.g. light from the active normal probe reflected onto the active angled probe, the resulting beat frequency was not considered. Future work can be performed to utilize the additional interference for redundant measurements, which ultimately drives down the overall uncertainty with weighted averaging. Lastly, the combined normal-transverse velocity state fed into the model was assumed to be fully established, i.e. both the longitudinal and shear wave had reached the free surface.

Single Measurement

$$\delta V_T = \sqrt{\left(\frac{dV_T}{dV^*}\delta V^*\right)^2 + \left(\frac{dV_T}{dV_N}\delta V_N\right)^2 + \left(\frac{dV_T}{d\alpha}\delta\alpha\right)^2 + \left(\frac{dV_T}{d\beta}\delta\beta\right)^2} \quad (2)$$

Direct Measurement

$$\delta V_T = \sqrt{\left(\frac{dV_T}{dV_1^*}\delta V_1^*\right)^2 + \left(\frac{dV_T}{dV_2^*}\delta V_2^*\right)^2 + \left(\frac{dV_T}{d\alpha_1}\delta\alpha_1\right)^2 + \left(\frac{dV_T}{d\alpha_2}\delta\alpha_2\right)^2} \quad (3)$$

Averaged Measurement

$$\delta V_T = \sqrt{\left(\frac{dV_T}{dV_{T,1}}\delta V_{T,1}\right)^2 + \left(\frac{dV_T}{dV_{T,2}}\delta V_{T,2}\right)^2} \quad (4)$$

RESULTS

The relative uncertainty in transverse velocity was plotted for each configuration as a function of probe angle, impact angle, and measurement uncertainty in particle velocity, Figure 3. Two vertical dashed lines are shown for each plot and represent the typical working range for an active and/or passive angled probe (15 – 30 degrees) based on a linearly diffuse surface treatment [8,9]. As probe angle goes from 0 to 90 degrees, the angled probes observe a

larger component of the transverse velocity, which causes a decrease in relative uncertainty for all configurations. Likewise, as impact angle increases from 15 to 25 degrees, a larger component of transverse velocity is expected at the free surface (relative to the magnitude of the normal velocity) and again decreases the relative uncertainty. Lastly, as the magnitude of particle velocity measurement uncertainty increases from 1% to 2.5% and 2.5% to 5%, a large increase in relative uncertainty is observed for all configurations. This quantity is directly related to the experimental setup and data processing through sampling rate, analysis window size, and signal to noise ratio [12]. It is apparent from figure 3 that any increase in particle velocity measurement uncertainty has a more significant effect on probe configurations that use passive probes. Conversely, configurations with active probes show that particle velocity measurement uncertainty has less of an effect on relative uncertainty in transverse velocity.

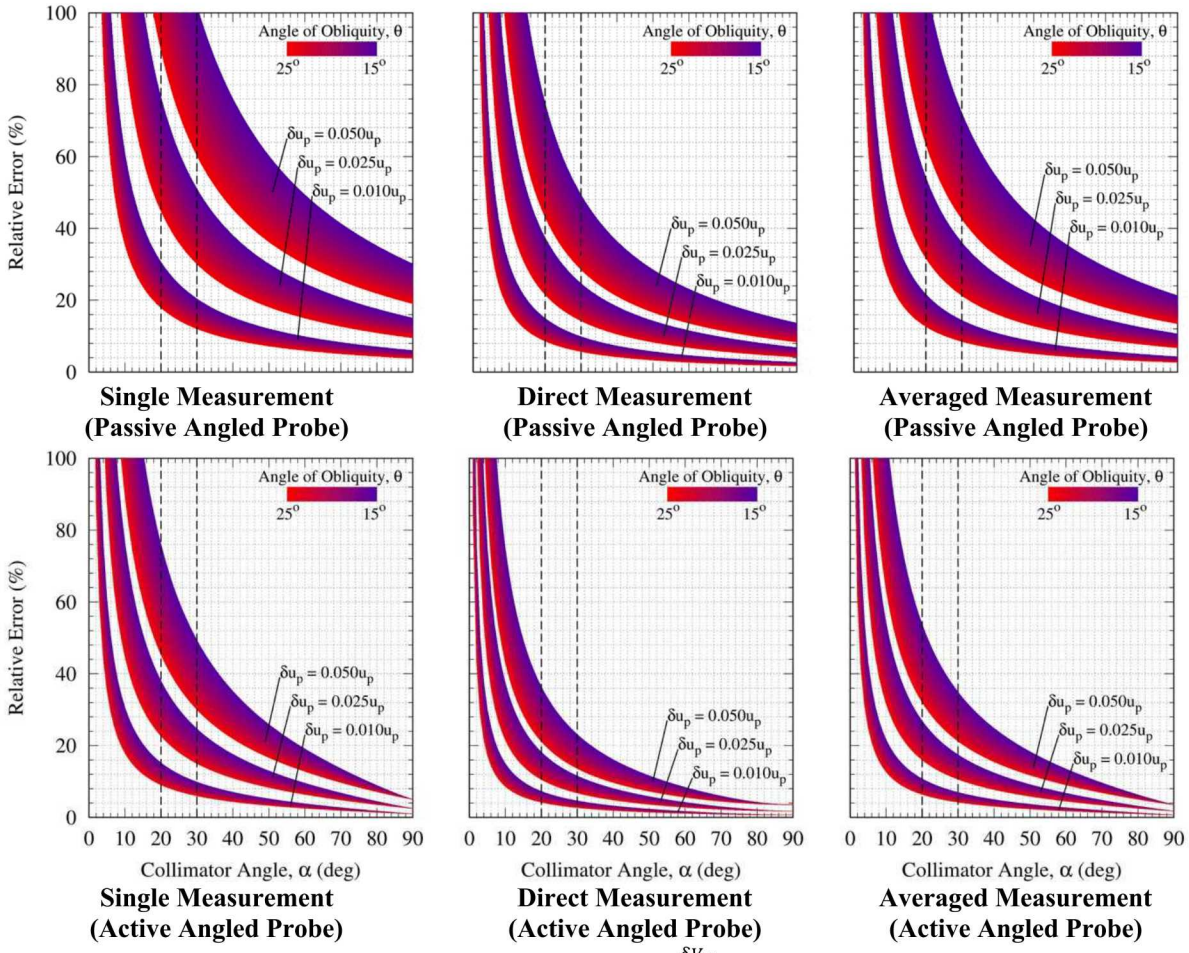

FIGURE 3 Relative error (uncertainty) in transverse velocity, $\frac{\delta V_T}{V_T}$, for each probe configuration when varying the collimator angle from $\alpha = 0 - 90°$, the angle of obliquity (angle of impact) from $\theta = 15 - 25°$, and percent error of particle velocity, $\delta u_p = 1.0\%, 2.5\%,$ and 5.0% as measured using PDV.

Comparing the results for active/passive angled probes in each of the three types of configurations, it can be concluded that any configuration using passive probes inherently has greater relative uncertainty in transverse velocity. Since each configuration was fed the same test data, this result is due purely to geometric influences on the apparent velocity equation. If each of the configurations are compared at the same particle velocity measurement uncertainty, the direct measurement configuration results in the lowest relative uncertainty in transverse velocity. The averaged measurement configuration is a close second, but suffers slightly due to the dependence of the calculated transverse velocity on not only the apparent velocity observed on an angled probe, but also the normal velocity observed on the normal probe. However, since the direct measurement configurations do not utilize heterodyne "upshifting" of the fundamental beat frequency, they produce a beat frequencies with magnitudes on the

order of MHz. Conversely, both single and averaged measurements allow for upshifting, which yields a beat frequency on the order of multiple GHz. The lower frequency in direct measurements results in less fringes per analysis window during the extraction of velocity magnitude from spectral content and, ultimately, larger uncertainty in the magnitude of observed particle velocity, δV^*.

CONCLUSIONS

This study outlines a framework for comparing different approaches to make transverse surface velocity measurements and compares them using relative uncertainty calculations. Each configuration was tested with the same synthetic data and across the same parameter sweep. Therefore, any advantages a certain configuration presents is due to geometric variations in the transverse velocity equation. Direct measurement configurations resulted in the lowest relative uncertainty for both active and passive angled probes. However, in actual experimental measurements, the number of fringes available in direct measurements of transverse velocity (without upshifting) is drastically lower compared to either single or averaged measurement configurations due to their upshifted beat frequencies. Further work to quantify measurement uncertainty due to this difference in fringe count per analysis window is necessary if a clear advantage is to be given to either direct or averaged measurements. Other considerations such as fiber optic component availability, surface preparation and types of light return, and desired measurement accuracy should all factor in when choosing the appropriate probe configuration.

ACKNOWLEDGEMENTS

The authors would like to thank Allen Dalton of DTRA for initial funding of this work through DTRA grant: HDTRAA1-15-1-0073, Scott Alexander, Chris Johnson, Christopher Neel, and Tracy Vogler. Sandia National Laboratories is a multi-mission laboratory managed and operated by National Technology & Engineering Solutions of Sandia, LLC, a wholly owned subsidiary of Honeywell International INC., for the U.S. Department of Energy's National Nuclear Security Administration under contract DE-NA0003525.

REFERENCES

1. K. S. Kim, R. J. Clifton, and P. Kumar, "A combined normal- and transverse-displacement interferometer with an application to impact of y-cut quartz," *J. Appl. Phys.*, vol. 48, no. 10, pp. 4132–4139, 1977.
2. A. S. Abou-Sayed *et al.*, "The Oblique-plate Impact Experiment," *Exp. Mech.*, vol. 16, no. 4, pp. 127–132, Apr. 1976.
3. Barker
4. O. T. Strand, L. V Berzins, D. R. Goosman, W. Kuhlow, P. D. Sargis, and T. L. Whitworth, "Velocimetry Using Heterodyne Techniques," 2004
5. D. H. Dolan, M. Elert, M. D. Furnish, W. W. Anderson, W. G. Proud, and W. T. Butler, "WHAT DOES 'VELOCITY' INTERFEROMETRY REALLY MEASURE?," in *AIP Conference Proceedings*, 2009, pp. 589–594.
6. G. Chen, D. Wang, J. Liu, J. Meng, S. Liu, and Q. Yang, "A novel photonic Doppler velocimetry for transverse velocity measurement," *Rev. Sci. Instrum.*, vol. 84, no. 1, 2013.
7. B. Zuanetti, T. Wang, and V. Prakash, "A compact fiber optics-based heterodyne combined normal and transverse displacement interferometer," *Rev. Sci. Instrum.*, vol. 88, no. 3, pp. 1–7, 2017.
8. C. R. Johnson, J. W. LaJeunesse, P. A. Sable, A. Dawson, A. Hatzenbihler, and J. P. Borg, "Photon Doppler velocimetry measurements of transverse surface velocities," *Rev. Sci. Instrum.*, vol. 89, no. 6, 2018.
9. J. W. LaJeunesse, "Dynamic Behavior of Granular Earth Materials Subjected to Pressure-Shear Loading," Marquette University, 2018.
10. C. Kettenbeil, M. Mello, M. Bischann, and G. Ravichandran, "Heterodyne transverse velocimetry for pressure-shear plate impact experiments," *J. Appl. Phys.*, vol. 123, no. 12, pp. 1–14, 2018.
11. D.D. Mallick, M. Zhao, B.T. Bosworth, B.E. Schuster, M.A. Foster, K.T. Ramesh, "A simple dual-beam time-multiplexed photon doppler velocimeter for pressure-shear plate impact experiments," *Exp. Mech.*, vol. 5 (1), pp. 41-49, 2018
12. D. H. Dolan, "Accuracy and precision in photonic doppler velocimetry," *Rev. Sci. Instrum.*, vol. 81, no. 5, 2010.